OXFORD Regenerative Biomaterials

Regenerative Biomaterials, 2022, **9**, rbac006
https://doi.org/10.1093/rb/rbac006
Advance Access Publication Date: 2 February 2022
Research article

Nitric oxide-releasing polyurethane/*S*-nitrosated keratin mats for accelerating wound healing

Jie Dou[1,†], Rong Yang[2,†], Xingxing Jin[1], Pengfei Li[1], Xiao Han[1], Lijuan Wang[1], Bo Chi[2,*], Jian Shen[1,*] and Jiang Yuan[1,*]

[1]Jiangsu Collaborative Innovation Center of Biomedical Functional Materials, Jiangsu Key Laboratory of Bio-functional Materials, School of Chemistry and Materials Science, Nanjing Normal University, Nanjing 210023, P.R. China and
[2]State Key Laboratory of Materials-Oriented Chemical Engineering, College of Food Science and Light Industry, Nanjing Tech University, Nanjing 211816, P.R. China

*Correspondence address. E-mail: bioalchem@yahoo.com (J.Y.); E-mail: chibo@njtech.edu.cn (B.C.); E-mail: jshen@njnu.edu.cn (J.S.)
†These two authors contributed equally to this work.

Abstract

Nitric oxide (NO) plays an important role in wound healing, due to its ability to contract wound surfaces, dilate blood vessels, participate in inflammation as well as promote collagen synthesis, angiogenesis and fibroblast proliferation. Herein, keratin was first nitrosated to afford *S*-nitrosated keratin (KSNO). As a NO donor, KSNO was then co-electrospun with polyurethane (PU). These as-spun PU/KSNO biocomposite mats could release NO sustainably for 72 h, matching the renewal time of the wound dressing. Moreover, these mats exhibited excellent cytocompatibility with good cell adhesion and cell migration. Further, the biocomposite mats exhibited antibacterial properties without inducing severe inflammatory responses. The wound repair *in vivo* demonstrated that these mats accelerated wound healing by promoting tissue formation, collagen deposition, cell migration, re-epithelialization and angiogenesis. Overall, PU/KSNO mats may be promising candidates for wound dressing.

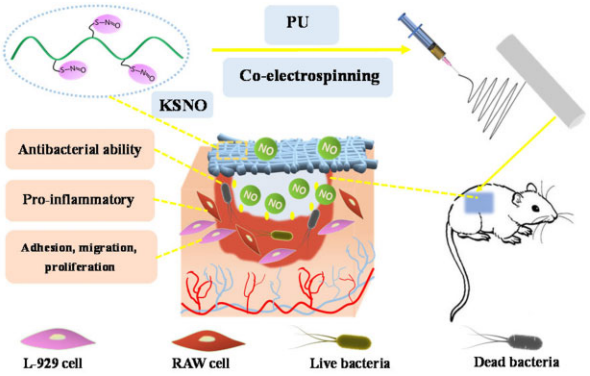

Keywords: keratin; nitric oxide; wound dressing; electrospinning; biocomposite

Introduction

As the largest single organ, skin is mostly exposed to damage more than any other part of the body. These damages vary from small cuts, which can be healed naturally in a couple of days, to severe third-degree burns, which can threaten life if medical intervention is not timely [1, 2]. Wound healing is crucial to the recovery of body integrity after injury, with the need to restore function and anatomical structure to a baseline level [3]. Wound healing is a dynamic and complex process that involves coagulation, inflammation, granulation, proliferation, matrix synthesis and deposition, fibrogenesis, angiogenesis, wound contraction and re-epithelialization [4, 5]. In most cases, it is a prodigious challenge in the clinic because the wound healing process immediately starts with the injury and might last for several months. Hence, rapid wound healing in an ideal local environment is pivotal [6].

Nitric oxide (NO) plays many critical physiological roles in the regulation and protection of numerous tissue and organ functions [7]. As a gasotransmitter, NO is responsible for promoting wound healing by re-epithelialization, improving angiogenesis through the expression of multiple growth factors and cytokines [8, 9]. Intriguingly, NO has excellent antibacterial capability as well. NO-donor loaded polymeric materials have generated significant interest in wound dressings, which are capable of releasing NO at controlled rates [10–18]. Won *et al.* [19] conjugated *N*-diazeniumdiolates with a tri-block copolymer, accelerating palatal wound healing. de Oliveira *et al.* [20] prepared poly(acrylic acid)/F127/*S*-nitrosoglutathione hydrogel, which was a potential platform for accelerating wound healing and treating chronic wounds. Seabra *et al.* [21] incorporated *S*-nitroso-mercaptosuccinic acid and silver nanoparticles into alginate hydrogel for topical antibacterial applications. However, a handful of NO donors are available on biomedical applications because most of synthetic donors are toxic and unstable.

Nanofibrous mats with high specific area and 3D structure are promising candidates for wound dressings [22, 23]. Bazmandeh *et al.* [24] electrospun chitosan-gelatin and chitosan-hyaluronic acid to resemble the fibrous/gel structure of natural skin extracellular matrix (ECM) wound healing properties. Yoo *et al.* [25]

Received: November 01, 2021. **Revised:** January 24, 2022. **Accepted:** January 24, 2022

fabricated adipocyte-derived stem cells/gelatins-poly(caprolactone) nanofibrils cell sheets, exhibiting more effective wound-healing efficiency. Schoenfisch *et al.* [26] incorperated low-molecular-weight NO donor with polymer to prolong NO release. Zhou *et al.* [27] prepared carboxyethyl chitosan/poly(vinyl alcohol) mats used as potential wound dressing for skin regeneration.

As a cytoskeletal scaffolding protein, keratin is essential for wound healing and tissue recovery. Till now, keratin-based wound dressings have been well developed [28–32]. In this study, S-nitrosated keratin (KSNO) was used as NO supply. The biomacromolecular NO donor of KSNO should has higher stability and lower cytotoxicity as compared to low-molecular synthetic NO donors. Then, KSNO was co-electrospun with polyurethane (PU) to afford PU/KSNO mats. The as-spun mats could release NO sustainably, thereby accelerating wound healing. The physicochemical and biological properties, such as hydrophilicity, cytocompatibility and antibacterial activity were characterized. Furthermore, the wound repair of PCL/KSNO mats *in vivo* was evaluated on Sprague-Dawley (SD) rats (Scheme 1).

Experimental

Materials

Pellets of thermoplastic PU (Mw = 70 000) were provided by Xianbang Technology Co., Ltd (Nanjing, China). 1,1,1,3,3,3-Hexafluoro-2-isopropanol (HFIP) and *tert*-butyl nitrite were provided by the Aladdin Company (Shanghai, China). Griess reagent was provided by Beyotime Institute of Biotechnology (Haimen, China). All other chemicals were used as received.

Synthesis of KSNO

The KSNO was developed by our lab [33]. In brief, the reduced keratins were extracted from human hair by the reduction method, followed by converting to S-nitrosothiols by the reaction with *tert*-butyl nitrite. Then, KSNO was purified under vacuum and stored in the dark for future use.

Fabrication of PU/KSNO mats by electrospinning

PU and KSNO were dissolved in HFIP to obtain polymer solutions at concentrations of 4 wt% with stirring at room temperature for electrospinning. To keep the good mechanical property, the mass ratio of PU to KSNO was 9 and 1. The mixed solution was electrospun via a 20 ml syringe with an 18 G metal needle at a flow rate of 2.0 ml/h. The parameters for the collector were maintained at a voltage of 20 kV and a collection distance of ~15 cm from the tip of the needle. The canary yellow fiber membranes were dried in a vacuum overnight at 37°C to remove the residue solvent before proceeding with other experiments.

NO release *in vitro*

To determine the NO release, the equal weight PU/KSNO mats (Φ15 mm) were immersed in phosphate-buffered saline (PBS) solution (2 ml, pH = 7.4) in the absence and presence of ascorbic acid (Asc, 250 μg/ml), respectively. At predetermined time intervals, the solution was collected and replaced with the corresponding solution. Afterward, 50 μl of collected supernatant of each sample was transferred into a 96-well plate, reacted with 100 μl Griess reagent, and incubated for another 15 min in the dark. The absorbance at 540 nm was measured using a microplate reader (BioTek ELx800, USA). Ultimately, the cumulative release of NO can be calculated according to the standard curve.

Cytotoxicity of PU and PU/KSNO mats

To evaluate the cytotoxicity of PU/KSNO mats and KSNO, an MTT assay was carried out with L-929 cells. Before biological assays, all mats were sterilized with ethanol 75% (V/V) for 30 min and then was fixed by the sterilized glass ring into the plates, followed by washing thrice with PBS. The cells were seeded on the surface of the pre-treated mats with a density of 5×10^4 cells/well and cultured in a humidified incubator with 95% air and 5% CO_2 at 37°C. Then, the PU/KSNO mats were added with 15 μl Asc (250 μg/ml) every 12 h. After culturing for 72 h, the supernatant was discarded and the samples were washed with PBS thrice to

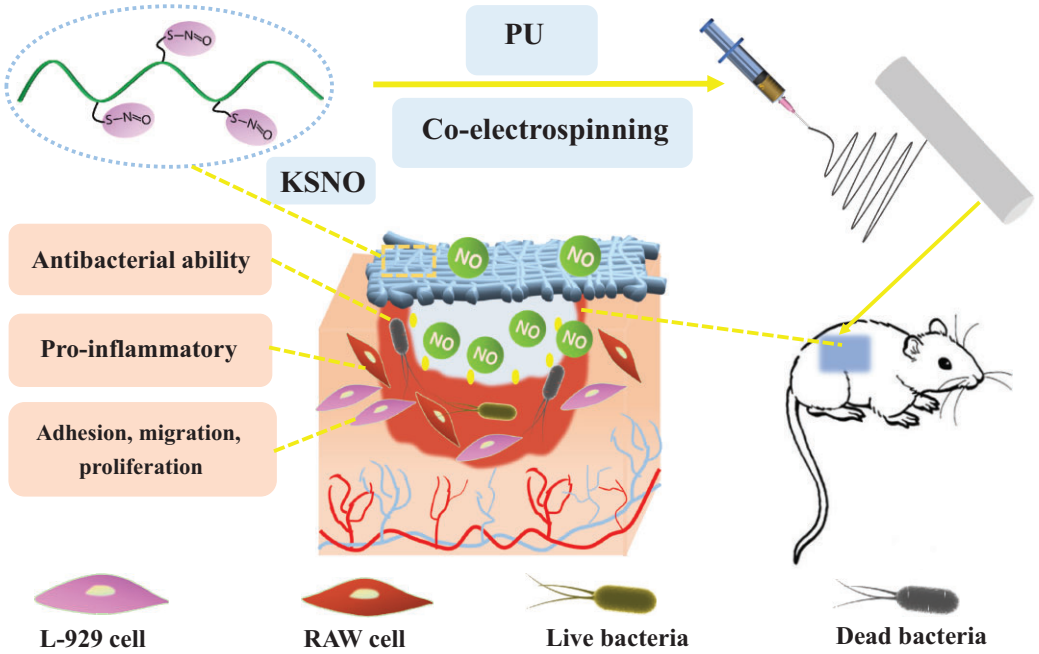

Scheme 1. Schematic preparation of PU/KSNO mats with NO release capacity for accelerating wound healing

remove non-attached cells. Dulbecco's Modified Eagles Media (1 ml) (DMEM, Hyclone) with 100 μl of MTT solution was added and incubated at 37°C for another 4 h. Then, the upper solvent was removed and the bluish-violet formazan crystals were dissolved in 500 μl of dimethyl sulfoxide (DMSO) for 30 min in dark and 100 μl of the solution in each well was transferred to a new 96-well plate, and the absorbance at 490 nm was measured with a microplate reader. To evaluate the KSNO toxicity, various concentrated KSNO solutions were prepared. The equal DMSO (1%, V/V) was added to improve the KSNO solubility. The effect of KSNO concentration on the cytotoxicity was tested with MTT assay for 3 days.

Cell migration assay

Cell migration assay is a simple and economical method to mimic cell migration *in vivo* to some extent. Cell migration assay was conducted with L-929 cells, representing the expansion of cell population on the surface. Before the test, the mat was cut into a square (2.5×2.5 cm^2), immersed with ethanol 75% (V/V), and exposed to the ultraviolet irradiation for 1 h on both sides for sterilization, followed by placed into a 6-well plate and fixed with sterilize stainless steel bar and then infiltrated with PBS. Then, PBS was removed and the stainless steel mold of a specific size was pressed onto the samples to form gaps. L-929 cells cultured in the petri dish were stained with Cell Tracker™ Green CMFDA dye (1.5×10^{-5} M) and incubated in a humidified atmosphere of 5% CO_2 at 37°C for 1 h. Subsequently, cells were digested and seeded at the 6-well plate at a density of 1.5×10^6 cells/ml in DMEM and 10% fetal bovine serum (FBS) and cultured at 37°C. After 4 h, the mold was removed and 15 μl of Asc (250 μg/ml) was added into PU and PU/KSNO groups and cultured for another 24 h. Correspondingly, the PU and PU/KSNO mats in the absence of Asc were set as controls. The photos of cells were taken using the inverted fluorescence microscope and the distance of cell migrated was measured using Image J software.

Antibacterial activity

The antibacterial activity of PU/KSNO mats against *Escherichia coli* was tested using the inhibition zone method. PU and PU/KSNO mats with 1.5 cm diameter were carefully removed from the aluminum foil and sterilized using 75% ethanol. The sterilized mats were gently placed onto the surface of Luria–Bertani agar plates triangularly with 10^4 CFUs/ml. A cotton ball saturated with Asc (250 μg/ml in PBS) was placed on the specimens. Incubated at 37°C for 24 h, the antibacterial activity of the sample was evaluated by measuring the zone of inhibition according to photos.

MTT method was also conducted to assess the antimicrobial activity. The round mats with a diameter of 1.5 cm were sterilized under UV light for 1 h (30 min for each side) and covered with 1 ml *E.coli* suspension (10^7 CFUs/ml) in a 24-well plate. For the PU/KSNO mats, the antimicrobial effect of NO from KSNO was conducted with and without Asc (250 μg/ml in PBS). After culturing for 24 h, 100 μl of MTT solution was added and incubated at 37°C for another 4 h. Then, the old medium was discarded, followed by the addition of 500 μl DMSO to dissolve the blue crystal. The optical density value at 490 nm was measured by a microplate reader.

Pro-inflammatory response test

RAW 264.7 cells (3×10^5 cells/cm^2 in DMEM supplemented with 10% FBS and 4 mM L-glutamine) were seeded in triplicate onto mats. The tumor necrosis factor-alpha (TNF-α) secreted for 24 h incubation was quantified with TNF-α ELISA kit. Cells stimulated with lipopolysaccharide (10 ng/ml, LPS) were used as a positive control. For the NO generation, the concentration of Asc was 3.75 μg/ml.

Animal models

All animal experiments were approved and instructed by the Animal Investigation Ethics Committee of Nanjing Tech University. All the SD rats (6 weeks, 160∼200 g, female) were fed with sterile water and standard chow. After anesthetizing with 3% pentobarbital sodium (0.2 ml/100g) and shaving dorsal hair with an electrical hair cutter, the full-thickness skin defects (1 cm diameter) were created on the upper back of each rat. The PU/KSNO mats were applied to the wounds, and cotton gauze and PU mats were used as controls. The wound dressing was replaced every 2 days. Asc concentration in human blood is about 15 μg/ml, which is much lower than that in our experiments (250 μg/ml). Therefore, all mats were immersed with Asc solution (1%) for 5 min before operation. The adsorbed Asc would act as a catalyst to generate NO for mats during wound treatment.

All rats were sacrificed after 14 days, and their fresh wound tissues were harvested and immersed in 4% formaldehyde tissue fixing fluid for 24 h. Then, the fixed wound tissue was embedded in paraffin for histological examination, including hematoxylin and eosin (H&E) and Masson's trichrome staining. Wound coverage percentage was measured by the software Image J and calculated by the formula:

$$\text{Woundcoverage}\ (\%) = A_t/A_0 \times 100\%,$$

where A_t and A_0 are the wound area at the time of the rats been sacrificed and the initial wound area, respectively.

Statistical analysis

The results are expressed as the means ± standard deviations. Statistical analysis was performed using Origin 8.5 (OriginLab, Northampton, MA). Significant differences were determined using one-way ANOVA. The data were considered statistically significant at $P < 0.05$.

Results and discussion

Electrospinning and characterization

Electrospinning is a favorable low-cost fabrication technique, particularly in skin tissue engineering and wound healing applications. The as-spun mats with mimicked ECM structure are capable to absorb large wound exudates, enable gas permeation, prevent wound dehydration and promote cell growth [34, 35]. Figure 1 presents the SEM micrographs and diameter distribution of electrospun PU and PU/KSNO mats. For each sample, three SEM images were analyzed, and at least 40 fibers were manually measured on each image and analyzed using Image J software. Smooth and uniform fibrous structures were well retained, except for a decrease in the mean diameter (544.8 ± 74.5 nm) when compared with that of the pristine PU (723.4 ± 155.9 nm). It may be ascribed to the incorporation of high-polar KSNO, leading to a smaller diameter.

Supplementary Fig. S1 shows ATR-FTIR spectra of nanofibrous mats. There were no apparent differences between them because KSNO was nearly embedded into the fibers completely. XPS analysis was conducted to characterize the chemical structure. The elemental compositions were calculated and shown in Supplementary Table S1. In Fig. 2A, bare PU shows a peak at

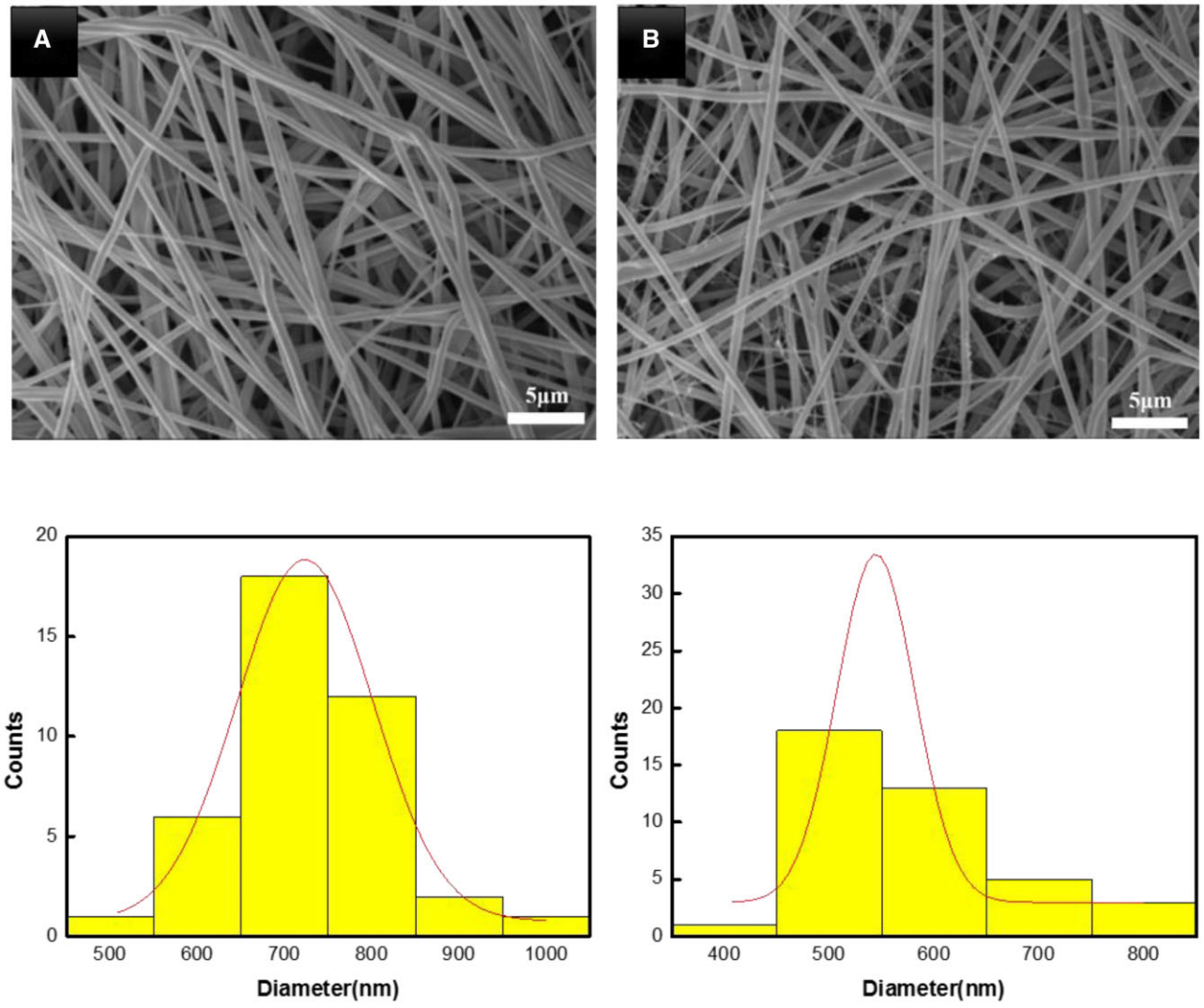

Figure 1. SEM images and fibrous diameter profile of PU (**A**) and PU/KSNO (**B**)

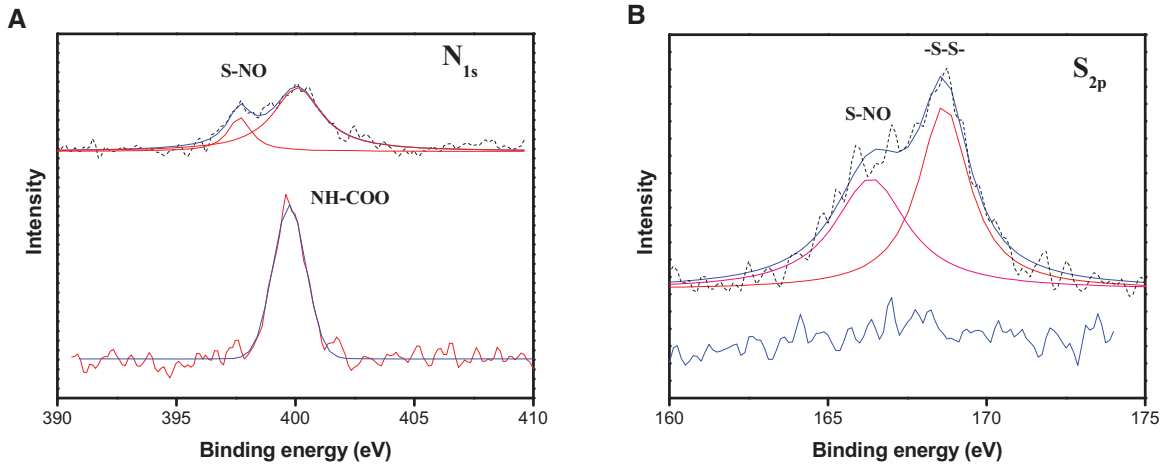

Figure 2. (**A**) High-resolution N_{1s} XPS spectra; (**B**) high-resolution S_{2p} XPS spectra of PU (lower) and PU/KSNO mats (upper)

399 eV, corresponding to its urethane structure. N_{1s} peaks for PU/KSNO mats were observed at 397 and 400 eV. Besides, N% at 397 eV was increased from 3.3% to 3.6%, which was contributed by KSNO. Compared to bare PU, the S_{2p} peak for PU/KSNO mats appeared at 166.4 eV (S–NO) and 168.7 eV (–S–S–) (Fig. 2B). There was a sudden appearance of sulfur about 1.4%. The increased N%

and S% for PU/KSNO compared to PU revealed the successful introduction of KSNO.

Traditional wound dressings mainly include natural or synthetic bandages, gauzes and cotton wool. Their main functions are to maintain the moist wound environment and absorb the excess exudates [36]. As depicted in Supplementary Fig. S2, the water contact angle reduced from 109.9 ± 2.8° to 39.1 ± 7.6°. It indicated that the hydrophilicity was improved largely after the introduction of KSNO, which could meet the demand in a moist environment for wound healing. In addition, the excellent hydrophilicity and 3D structure as well as the porosity of fibrous mats would have good wound exudate absorption capacity. The SEM images showed that PU and PU/KSNO mats did not degrade seriously with trypsin for 5 days (Supplementary Fig. S3).

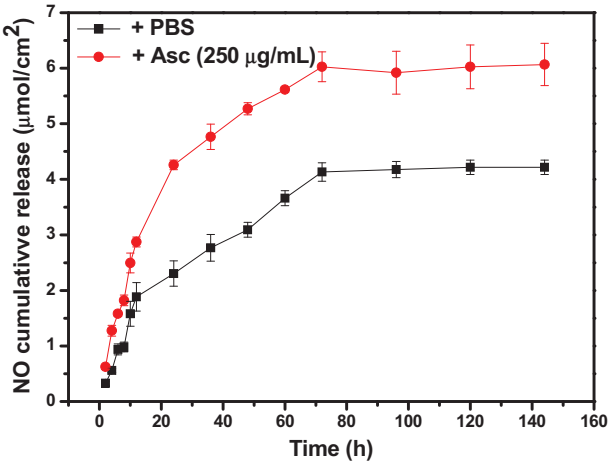

Figure 3. The cumulative release of NO from PU/KSNO mats in asc solution (250 μg/ml) and PBS buffer, respectively ($n = 3$)

NO release *in vitro*

KSNO was prepared by the S-nitrosation method, that was, converting the –SH to –SNO group. This method was simple and the product was easy to be purified. It was reported the NO-releasing wound dressings could effectively accelerate wound healing and inhibit the formation of scars [37]. Figure 3 presents the accumulated release of NO from PU/KSNO mats in PBS buffer and Asc solution, respectively. These mats could continuously release NO in both Asc and PBS solutions up to 3 days, while performed the accelerated release under Asc condition. As a nucleophile, Asc reacts with S-nitrosothiols and releases NO through electrophilic nitrosation, accompanied by the formation of a free thiol and dehydroascorbic acid [38, 39]. The NO release time matches the renewal time of the wound dressing very well because the wound needs to redress every 2∼3 days in general. The releasing NO helps clear bacterial infection in the initial stage of the wound to begin the satisfactory wound healing process [40, 41].

Cell viability

Cytocompatibility is a prerequisite for KSNO and PU/KSNO mats used as a wound dressing. Thus, MTT assay was carried out to test the cell viability (Fig. 4). To increase the solubility of KSNO, KSNO was dissolved with DMSO and diluted to each well. The toxicity of KSNO showed a concentration-dependent feature (Fig. 4A). The cell viability was reduced with the increasing concentration. There was nearly no toxicity as its concentration was higher than 250 μg/ml, indicating their good cytocompatibility. Cytocompatibility of PU/KSNO mats in Asc solution (250 μg/ml) and PBS buffer was also conducted. The cell viability on the PU mats was ∼80%, which could be considered non-cytotoxic (Fig. 4B). Furthermore, the cell viability on the PU/KSNO mats with and without Asc was significantly higher than that on the PU mats, indicating the released NO had no cytotoxicity *in vitro* and even promoted cell growth

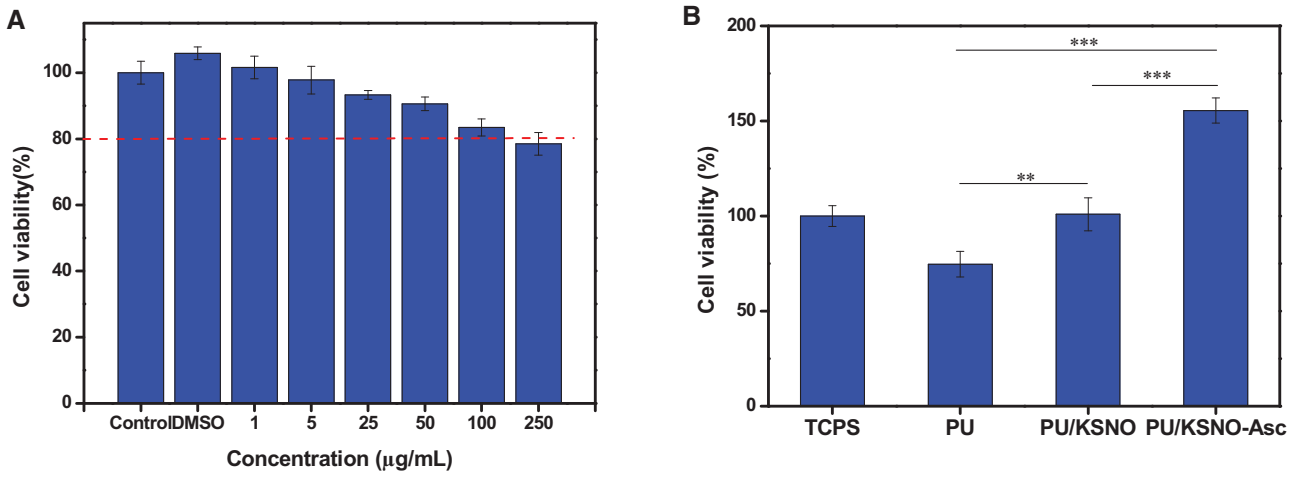

Figure 4. (**A**) Cell viability of KSNO as the functions of concentrations after incubation with L-929 cells for 3 days($n = 5$); (**B**) cell viability of L-929 cells after incubation for 3 days using tissue culture polystyrene as a control ($n = 5$, ** represents $P < 0.01$; *** represents $P < 0.001$)

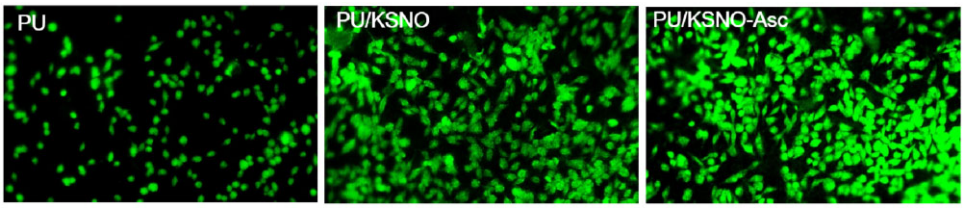

Figure 5. Fluorescence images of L-929 seeded on the PU, PU/KSNO, and PU/KSNO-Asc mats for 6 h culture (×10)

and proliferation [42, 43]. It may be explained that NO released from donors accelerated the fibroblast proliferation and leaded to collagen deposition thus resulting in faster wound healing [44]. Interestingly, the cell viability of the PU/KSNO-Asc group was significantly superior to that of the PU/KSNO group. Previously, KSNO was proven to have lower cytotoxicity than that of GSNO [45].

Cell adhesion

Keratin contains cell-binding motifs, such as leucine–aspartic acid–valine, glutamic acid– aspartic acid–serine and arginine–glycine–aspartic acid, which imitate the environment of the ECM to accelerate the adhesion and proliferation of fibroblasts [46, 47]. Observed by fluorescence microscopy, some cells with round appearance adhered to PU mats (Fig. 5). For PU/KSNO mats, more cells were attached as compared to PU mats due to the biocompatible KSNO. Regarding PU/KSNO-Asc mats, a large number of cells with a spreading phenotype were adhered. These results were in line with the results of cell viability. Supplementary Fig. S4 shows SEM images of HUVECs on the PU and PU/KSNO mats for 6 h adhesion. The results were consistent with the above conclusions.

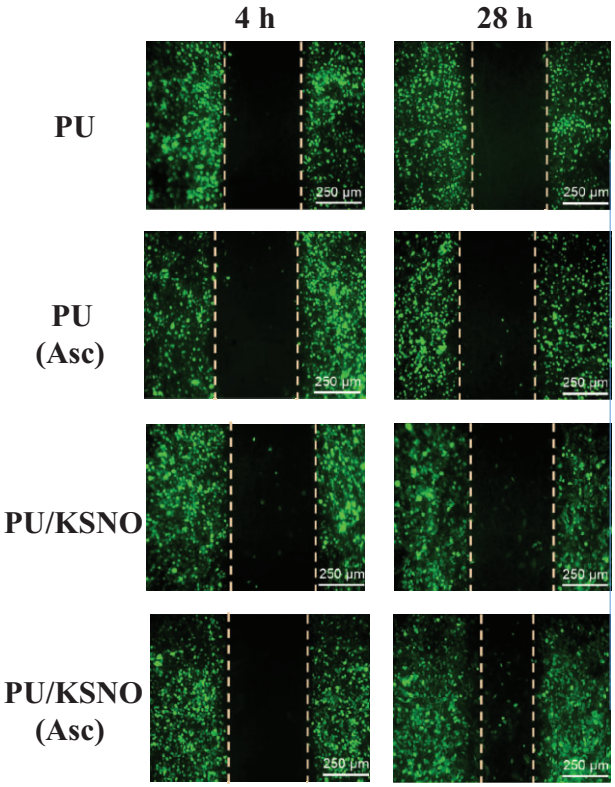

Figure 6. Cell migration images of L-929 cells at 4 and 28 h

Cell migration assay

The cell migration assay was used to *in vitro* evaluate the wound healing potential of the PU/KSNO dressings. As depicted in Figs 6 and 7A, the images of the distance of L-929 cell migration were taken at 4 and 28 h. There is no significant difference between PU, PU-Asc and PU/KSNO groups. However, the fibroblasts exposed to the PU/KSNO-Asc group exhibited much faster cell migration. It was because KSNO could release NO largely with the catalysis of Asc under moist and physiological temperature conditions, resulting in faster cell migration. The *in vitro* data of fibroblast proliferation and migration provide evidence for supporting wound healing [13].

Antibacterial activity

Bacterial adhesion to the artificial surfaces is considered as the pre-determining step during biofouling and biofilm formation [48, 49]. The antibacterial activities of various mats were evaluated by the agar plate diffusion method against gram-negative *E.coli* (Supplementary Fig. S5). From the MTT results, PU and PU/KSNO mats did not show an obvious antibacterial effect. On the contrary, PU/KSNO-Asc mats displayed significant inhibition of bacterial growth due to the catalytic release of NO (Fig. 7B). It indicated the excellent antibactericial ability of PU/KSNO was improved by the accelerated release of NO in the presence of Asc. The possible antibacterial mechanisms of NO include deamination of bacterial DNA, oxidation of proteins and inhibition of metabolic enzymes in bacteria [50, 51]. Asc ranged from 0.04 to 0.4 mg/ml has a bactericidal ability [52]. Herein, the used Asc was only 3.75 μg/ml, which was too low to exert bactericidal activity.

Pro-inflammatory response

The secreted TNF-α by RAW 264.7 cells cultured on mats was measured to evaluate the inflammatory response. As shown in

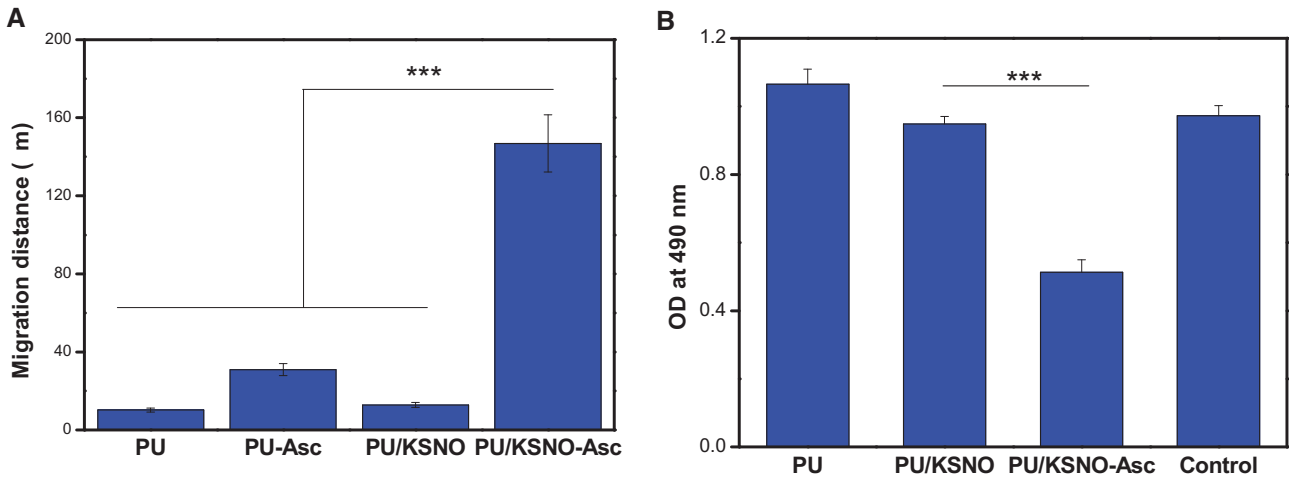

Figure 7. (**A**) Cell migration distance of L-929 cells on mats for 24 h ($n = 3$, ***, $P < 0.001$); (**B**) MTT results of *E.coli* cultured on mats for 24 h ($n = 5$, ***, $P < 0.001$)

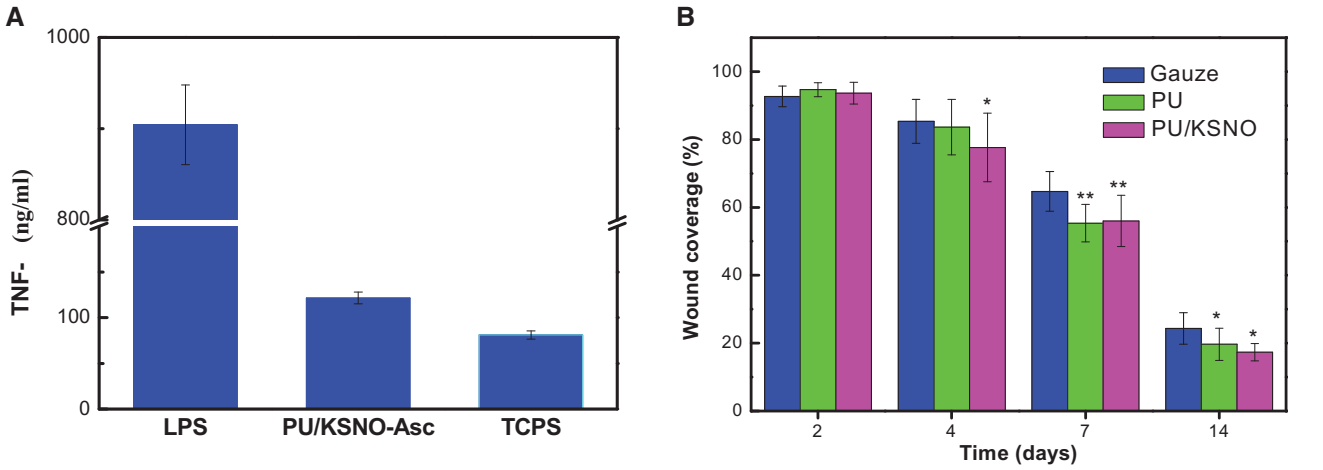

Figure 8. (**A**) TNF-α production by RAW264.7 macrophages seeded on mats for 24 h ($n = 5$); (**B**) wound coverage on animal models in gauze, PU mats and PU/KSNO mats; *, $P < 0.05$; **, $P < 0.01$ vs control ($n = 3$ for each group at each time point)

Fig. 8A, the level of TNF-α secretion was markedly lower than that stimulated with LPS. The TNF-α level for PU/KSNO-Asc group was slightly higher than that of the negative group. The results are in line with a report that NO would increase the production of TNF-α in mouse-cultured macrophages [53]. It is worth emphasizing that the slight inflammatory response plays a significant role in removing debris and protecting against pathogens at the implantation site [54].

Acceleration of wound healing

All mats were immersed with Asc solution (1%) for 5 min before wound treatment because Asc can catalyze NO release from mats. To test wound healing efficiency, the full-thickness skin defects on SD rats' models were conducted. The wound was photographed on Days 0, 2, 4, 7 and 14. As shown in Supplementary Fig. S6, the mats had a great difference in wound repair from *in vivo* experimental models. It seemed that PU mats had a better promotion effect due to their porous structures. In comparison, the wound contraction could be significantly improved after the treatment with PU/KSNO mats. Fig. 8B is a quantitative evaluation of wound healing in different groups on Days 2, 4, 7 and 14. The wound coverage of PU/KSNO mats was lower than 15% on Day 14, while that for PU and gauze groups was higher than 20%. These results exhibited that the wound healing efficiency of PU/KSNO mats was better than the controls.

The histological stain was used to evaluate the wound healing progress as well as investigate the skin tissue regeneration and collagen deposition. From the H&E staining and Masson staining in different groups, the thickness of the regenerative tissues was quite different among the three groups (Fig. 9). The thickness of the regenerative tissue for PU/KSNO group was the highest compared with the other groups and almost consistent with that of native tissues. Through the histological staining, it was found that the regenerative tissues contained mature blood vessels, thickened epidermis and a high density of microvessels in PU/KSNO groups. It was because the released NO from PU/KSNO mats improved angiogenesis and promoted wound healing progress. Angiogenesis is critical for wound healing because blood vessels can carry oxygen and nutrients to the wound [55]. As a signaling molecule, NO is responsible for promoting wound healing by re-epithelialization, improving angiogenesis through the expression of multiple growth factors and cytokines [56, 57].

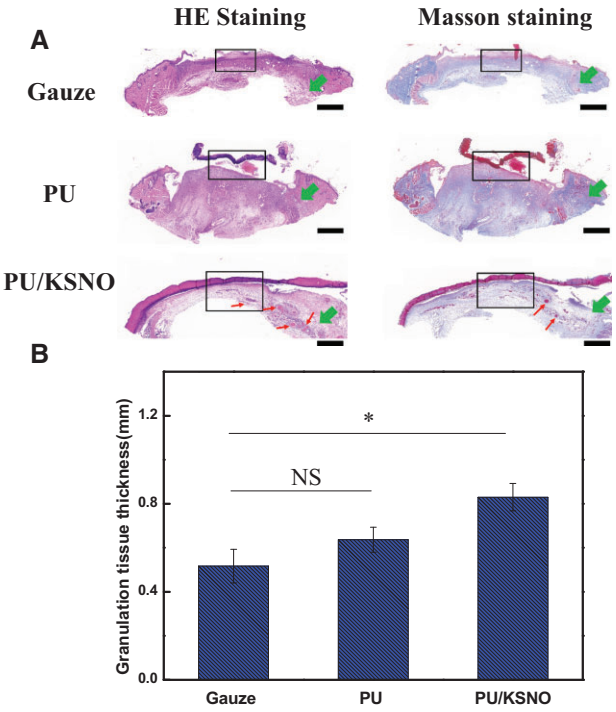

Figure 9. Histology of regenerative tissues. (**A**) H&E staining and Masson staining in gauze groups, PU mats groups and PU/KSNO mats groups. Black frameworks: regenerative tissues, green arrows: native tissues, red arrow: blood vessel, scale bar is 1 mm; (**B**) the thickness of regenerative tissues in different groups ($n = 3$). ns, not significant; *, $P < 0.05$; **, $P < 0.01$.

In the process of wound healing, the formation of blood vessels is very important because wound healing needs enough nutrients, which are transported through the blood to the wound. Too little new blood vessel formation will delay wound healing. Meanwhile, a much larger number of collagen fibers were observed in the PU/KSNO mats treated groups, and the phenomenon revealed that PU/KSNO mats also had a positive effect on promoting collagen deposition. Besides, the granulation tissues were much thicker in the PU/KSNO mats group than in the other two groups. It proved the released NO by PU/KSNO mats greatly promoted granulation tissue formation and collagen deposition,

resulting in accelerated wound recovery [19, 38, 58]. Overall, these results demonstrated that PU/KSNO mats possessed a great therapeutic effect by promoting granulation tissue regeneration and collagen deposition.

Conclusions

In summary, the NO donor of KSNO was used as NO supply and then incorporated with PU to produce PU/KNSO mats for wound dressing. These mats could release NO sustainably for 72 h, matching the renewal time of the wound dressing. The biocomposite mats promoted cell viability and exhibited antibacterial properties due to the sustained release of NO. More importantly, these mats could accelerate wound healing on a rat wound repair model by promoting tissue formation, collagen deposition, cell migration, re-epithelialization and angiogenesis. Overall, all results validated that PU/KSNO mats had the potential to be wound dressings for skin repairing.

Supplementary data

Supplementary data are available at *REGBIO* online.

Acknowledgments

J.Y. acknowledges financial support from Jiangsu Higher Education Institutions (19KJA310001 and PAPD).

Conflict of interest statement. None declared.

Author contributions

J.D. (conceptualization, investigation and original draft preparation), R.Y. (investigation and original draft preparation), X.J. (investigation), P.L. (resources and validation), X.H. (validation), L.W. (validation), B.C. (supervision), J.S. (supervision) and J.Y. (supervision, project administration, funding acquisition, review and editing).

References

1. Atiyeh BS, Gunn SW, Hayek SN. State of the art in burn treatment. *World J Surg* **2005**;29:131–48.
2. Blais M, Parenteau-Bareil R, Cadau S, Berthod F. Concise review: tissue-engineered skin and nerve regeneration in burn treatment. *Stem Cells Transl Med* **2013**;2:545–51.
3. Broughton G, Janis JE, Attinger CE. The basic science of wound healing. *Plast Reconstr Surg* **2006**;117:12S–34S.
4. Hamdan S, Pastar I, Drakulich S, Dikici E, Tomic-Canic M, Deo S, Daunert S. Nanotechnology-driven therapeutic interventions in wound healing: potential uses and applications. *ACS Cent Sci* **2017**;3:163–75.
5. Lisovsky A, Chamberlain MD, Wells LA, Sefton MV. Cell interactions with vascular regenerative MAA-based materials in the context of wound healing. *Adv Healthc Mater* **2015**;4:2375–87.
6. Guo S, DiPietro LA. Factors affecting wound healing. *J Dent Res* **2010**;89:219–29.
7. Ignarro LJ. Nitric oxide: a unique endogenous signaling molecule in vascular biology (Nobel Lecture). *Angew Chem Int Ed* **1999**; 38:1882–92.
8. Malone-Povolny MJ, Maloney SE, Schoenfisch MH. Nitric oxide therapy for diabetic wound healing. *Adv Healthcare Mater* **2019**; 8:1801210.
9. Kim HS, Sun XY, Lee JH, Kim HW, Fu XB, Leong KW. Advanced drug delivery systems and artificial skin grafts for skin wound healing. *Adv Drug Deliv Rev* **2019**;146:209–39.
10. Zhang Y, Tang K, Chen B, Zhou S, Li N, Liu Ch, Yang J, Lin R, Zhang T, He WA. Polyethylenimine-based diazeniumdiolate nitric oxide donor accelerates wound healing. *Biomater Sci* **2019**;7:1607–16.
11. Kim JO, Noh JK, Thapa RK, Hasan N, Choi M, Kim JH, Lee JH, Ku SK, Yoo JW. Nitric oxide-releasing chitosan film for enhanced antibacterial and in vivo wound-healing efficacy. *Int J Biol Macromol* **2015**;79:217–25.
12. Worley BV, Soto RJ, Kinsley PC, Schoenfisch MH. Active release of nitric oxide-releasing dendrimers from electrospun polyurethane fibers. *ACS Biomater Sci Eng* **2016**;2:426–37.
13. Pant J, Pedaparthi S, Hopkins SP, Goudie MJ, Douglass ME, Handa H. Antibacterial and cellular response toward a gasotransmitter-based hybrid wound dressing. *ACS Biomater Sci Eng* **2019**;5:4002–12.
14. Schanuel FS, Santos KSR, Monte-Alto-Costa A, de Oliveira MG. Combined nitric oxide-releasing poly(vinyl alcohol) film/F127 hydrogel for accelerating wound healing. *Colloids Surf B Biointerfaces* **2015**;130:182–91.
15. Ma XM, Cheng Y, Jian H, Feng YL, Chang Y, Zheng RX, Wu XQ, Wang L, Li X, Zhang HY. Hollow, rough, and nitric oxide-releasing cerium oxide nanoparticles for promoting multiple stages of wound healing. *Adv Healthcare Mater* **2019**;8:1900256.
16. Povoa VCO, dos Santos GJVP, Picheth GF, Jara CP, da Silva LCE, de Araujo EP, de Oliveira MG. Wound healing action of nitric oxide-releasing self-expandable collagen sponge. *J Tissue Eng Regen Med* **2020**;14:807–18.
17. Zou FX, Wang Y, Zheng YD, Xie Y, Zhang H, Chen J, Hussain MI, Meng H, Peng J. A novel bioactive polyurethane with controlled degradation and L-Arg release used as strong adhesive tissue patch for hemostasis and promoting wound healing. *Bioact Mater* **2022**. doi:10.1016/j.bioactmat.2022.01.009.
18. Thi TTH, Lee Y, Thi PL, Park KD. Nitric oxide-releasing injectable hydrogels with high antibacterial activity through in situ formation of peroxynitrite. *Acta Biomater* **2018**;67:66–78.
19. Won J, Shin J, Kim J, Kim W, Ryu J, Shim J. Multi-functional effects of a nitric oxide-conjugated copolymer for accelerating palatal wound healing. *Mater Sci Eng C* **2021**;125:112090.
20. Champeau M, Povoa V, Militao L, Cabrini FM, Picheth GF, Meneau F, Jara CP, de Araujo EP, de Oliveira MG. Supramolecular poly(acrylic acid)/F127 hydrogel with hydration-controlled nitric oxide release for enhancing wound healing. *Acta Biomater* **2018**;74:312–25.
21. Urzedo AL, Goncalves MC, Nascimento MHM, Lombello CB, Nakazato G, Seabra AB. Cytotoxicity and antibacterial activity of alginate hydrogel containing nitric oxide donor and silver nanoparticles for topical applications. *ACS Biomater Sci Eng* **2020**;6:2117–34.
22. Choi JS, Leong KW, Yoo HS. In vivo wound healing of diabetic ulcers using electrospun nanofibers immobilized with human epidermal growth factor (EGF). *Biomaterials* **2008**;29:587–96.
23. Ramanathan G, Sobhanadhas LSS, Jeyakumar GFS, Devi V, Sivagnanam UT, Fardim P. Fabrication of biohybrid cellulose acetate-collagen bilayer matrices as nanofibrous spongy dressing material for wound-healing application. *Biomacromolecules* **2020**;21:2512–24.
24. Bazmandeh AZ, Mirzaei E, Fadaie M, Shirian S, Ghasemi Y. Dual spinneret electrospun nanofibrous/gel structure of chitosan-gelatin/chitosan-hyaluronic acid as a wound dressing: in-vitro and in-vivo studies. *Int J Biol Macromol* **2020**;162:359–73.

25. Pham-Nguyen OV, Shin JU, Kim H, Yoo HS. Self-assembled cell sheets composed of mesenchymal stem cells and gelatin nanofibers for the treatment of full-thickness wounds. *Biomater Sci* **2020**;8:4535–44.
26. Coneski PN, Nash JA, Schoenfisch MH. Nitric oxide-releasing electrospun polymer microfibers. *ACS Appl Mater Interfaces* **2011**;3:426–32.
27. Zhou YS, Yang DZ, Chen XM, Xu Q, Lu FM, Nie J. Electrospun water-soluble carboxyethyl chitosan/poly(vinyl alcohol) nanofibrous membrane as potential wound dressing for skin regeneration. *Biomacromolecules* **2008**;9:349–54.
28. Wang YF, Li PF, Xiang P, Lu JT, Yuan J, Shen J. Electrospun polyurethane/keratin/AgNP biocomposite mats for biocompatible and antibacterial wound dressings. *J Mater Chem B* **2016**;4:635–48.
29. Konop M, Czuwara J, Klodzinska E, Laskowska AK, Sulejczak D, Damps T, Zielenkiewicz U, Brzozowska I, Sureda A, Kowalkowski T, Schwartz RA, Rudnicka L. Evaluation of keratin biomaterial containing silver nanoparticles as a potential wound dressing in full-thickness skin wound model in diabetic mice. *J Tissue Eng Regen Med* **2020**;14:334–46.
30. Giuri D, Barbalinardo M, Sotgiu G, Zamboni R, Nocchetti M, Donnadio A, Corticelli F, Valle F, Gennari CGM, Selmin F, Posati T, Aluigi A. Nano-hybrid electrospun non-woven mats made of wool keratin and hydrotalcites as potential bio-active wound dressings. *Nanoscale* **2019**;11:6422–30.
31. Singaravelu S, Ramanathan G, Muthukumar T, Raja MD, Nagiah N, Thyagarajan S, Aravinthan A, Gunasekaran P, Natarajan TS, Selva GVNG, Kim JH, Sivagnanam UT. Durable keratin-based bilayered electrospun mats for wound closure. *J Mater Chem B* **2016**;4:3982–97.
32. Yuan J, Geng J, Xing ZC, Shim KJ, Han I, Kim JC, Kang IK, Shen J. Novel wound dressing based on nanofibrous PHBV-keratin mats. *J Tissue Eng Regen Med* **2015**;9:1027–35.
33. Wan XZ, Liu S, Xin XX, Li PF, Dou J, Han X, Kang IK, Yuan J, Chi B, Shen J. S-nitrosated keratin composite mats with no release capacity for wound healing. *Chem Eng J* **2020**;400:125964.
34. Ekambaram R, Dharmalingam S. Fabrication and evaluation of electrospun biomimetic sulphonated peek nanofibrous scaffold for human skin cell proliferation and wound regeneration potential. *Mater Sci Eng C* **2020**;115:111150.
35. Kurtz SM, Devine JN. PEEK biomaterials in trauma, orthopedic, and spinal implants. *Biomaterials* **2007**;28:4845–69.
36. Zahedi P, Rezaeian I, Ranaei-Siadat SO, Jafari SH, Supaphol P. A review on wound dressings with an emphasis on electrospun nanofibrous polymeric bandages. *Polym Adv Technol* **2010**;21:77–95.
37. Kang Y, Kim J, Lee YM, Im S, Park H, Kim WJ. Nitric oxide-releasing polymer incorporated ointment for cutaneous wound healing. *J Control Release* **2015**;220:624–30.
38. Williams DLH. The chemistry of S-nitrosothiols. *Acc Chem Res* **1999**;32:869–76.
39. Holmes AJ, Williams DLH. Reaction of ascorbic acid with S-nitrosothiols: clear evidence for two distinct reaction pathways. *J Chem Soc Perkin Trans 2* **2000**;8:1639–44.
40. Seabra AB, Duran N. Nitric oxide-releasing vehicles for biomedical applications. *J Mater Chem* **2010**;20:1624–37.
41. Jones ML, Ganopolsky JG, Labbe A, Wahl C, Prakash S. Antimicrobial properties of nitric oxide and its application in antimicrobial formulations and medical devices. *Appl Microbiol Biotechnol* **2010**;88:401–7.
42. Pant J, Goudie MJ, Hopkins SP, Brisbois EJ, Handa H. Tunable nitric oxide release from s-nitroso-n-acetylpenicillamine via catalytic copper nanoparticles for biomedical applications. *ACS Appl Mater Interfaces* **2017**;9:15254–64.
43. Goudie MJ, Brisbois EJ, Pant J, Thompson A, Potkay JA, Handa H. Characterization of an s-nitroso-n-acetylpenicillamine–based nitric oxide releasing polymer from a translational perspective. *Int J Polym Mater* **2016**;65:769–78.
44. Han G, Nguyen LN, Macherla C, Chi YL, Friedman JM, Nosanchuk JD, Martinez LR. Nitric oxide–releasing nanoparticles accelerate wound healing by promoting fibroblast migration and collagen deposition. *Am J Pathol* **2012**;180:1465–73.
45. Li PF, Jin DW, Dou J, Wang LJ, Wang YF, Jin XX, Han X, Kang IK, Yuan J, Shen J, Yin M. Nitric oxide-releasing poly(ε-caprolactone)/S-nitrosylated keratin biocomposite scaffolds for potential small-diameter vascular grafts. *Int J Biol Macromol* **2021**;189:516–27.
46. Rouse JG, Van Dyke ME. A review of keratin-based biomaterials for biomedical applications. *Materials* **2010**;3:999–1014.
47. Wang YF, Zhang WW, Yuan J, Shen J. Differences in cytocompatibility between collagen, gelatin and keratin. *Mater Sci Eng C* **2016**;59:30–4.
48. May RM, Magin CM, Mann EE, Drinker MC, Fraser JC, Siedlecki CA, Brennan AB, Reddy ST. An engineered micropattern to reduce bacterial colonization, platelet adhesion and fibrin sheath formation for improved biocompatibility of central venous catheters. *Clin Transl Med* **2015**;4:9.
49. Wang Y, Wang C, Xie Y, Yang Y, Zheng YD, Meng H, He W, Qiao K. Highly transparent, highly flexible composite membrane with multiple antimicrobial effects used for promoting wound healing. *Carbohydr Polym* **2019**;222:114985.
50. Fang FC. Perspectives series: host/pathogen interactions. mechanisms of nitric oxide-related antimicrobial activity. *J Clin Invest* **1997**;99:2818–25.
51. Dai TH, Tanaka M, Huang YY, Hamblin MR. Chitosan preparations for wounds and burns: antimicrobial and wound-healing effects. *Expert Rev anti Infect Ther* **2011**;9:857–79.
52. Tabak M, Armon R, Rosenblat G, Stermer E, Neeman I. Diverse effects of ascorbic acid and palmitoyl ascorbate on helicobacter pylori survival and growth. *FEMS Microbiol Lett* **2003**;224:247–53.
53. Marcinkiewicz J, Grabowska A, Chain B. Nitric oxide upregulates the release of inflammatory mediators by mouse macrophages. *Eur J Immunol* **1995**;25:947–51.
54. Boni BOO, Lamboni L, Souho T, Gauthier M, Yang G. Immunomodulation and cellular response to biomaterials: the overriding role of neutrophils in healing. *Mater Horiz* **2019**;6:1122–37.
55. Tonnesen MG, Feng XD, Clark RAF. Angiogenesis in wound healing. *J Invest Derm Symp* **2000**;5:40–6.
56. Fatima AD, Modolo LV, Sanches ACC, Porto RR. Wound healing agents: the role of natural and non-natural products in drug development. *Mini Rev Med Chem* **2008**;8:879–88.
57. Rizk M, Witte MB, Barbul A. Nitric oxide and wound healing. *World J Surg* **2004**;28:301–6.
58. Witte MB, Thornton FJ, Efron DT, Barbul A. Enhancement of fibroblast collagen synthesis by nitric oxide. *Nitric Oxide Biol Chem* **2000**;4:572–82.